

Preparation and Structural Properties of Manganese Substituted cobalt Nano Ferrites By Citrate-Gel Auto Combustion Method

B.Kiran Kumar¹, D.Ravikumar¹, D.Ravinder^{2*}, Ch.Abraham Lincoln^{1*}.

1.Department of Chemistry, Osmania University, Hyderabad 500007, Telangana, India.

2.Department of Physics, Osmania University, Hyderabad 500007, Telangana, India

Abstract: Nano sized particles of manganese doped cobalt nano ferrites having general formula $Mn_xCo_{1-x}Fe_2O_4$ (where $x=0.0, 0.2, 0.4, 0.6, 0.8, 1.0$) were prepared by the citrate gel method at low temperature ($180^\circ C$). The synthesized powders were sintered at $500^\circ C$ for 4 hours. The crystal structure characterization of the sintered powders were carried out by using X-ray diffraction (XRD). The X-Ray diffraction analysis confirmed the formation of single phase cubic spinel structure. The average particle size of the synthesized powders was 11 to 33nm. The surface morphology were studied by Scanning Electron Microscopy (SEM) which revealed the formation of largely agglomerated nano particles. Lattice parameter, X-ray density, experimental density, porosity of the samples were calculated. The observed results can be discussed in this paper on the basis of composition.

I. Introduction

The study of nano crystalline material is a subject of considerable interest, both for the scientific value of understanding the unique properties of materials that have relevance to condensed matter studies and for the technological significance of enhancing the performance of existing materials [1,2]. Because of the large surface-to-volume ratios and quantum-size effect, their properties and structural stability are very different to those of their bulk counterpart [3,4] because of their novel properties and technological applications especially when the size of the particle approaches to the nanometer scale are very useful. A significant motivation of current research into nanometer sized materials is the need to develop an understanding of the structure-property relationship sensitive to preparation method. Commonly used ferrites are primarily classified into three types: spinels, hexagonal ferrites, and garnets according to their primary crystal lattice. Generally, ferrimagnetism arises from the anti parallel alignment of the magnetic moments on transition metal ions, present on different magnetic sub lattices. The origin of the anti parallel coupling can be explained by super-exchange of valence electrons between the filled p-orbitals of O^{2-} and unfilled d-orbitals of the transition metal cations. In ferrites, Fe^{3+} serves as the trivalent cation. Generally, the structure of spinel ferrites could be described with the $(M_{1-x}^{2+}Fe_x^{3+})[M_x^{2+}Fe_{1-x}^{3+}]O_4$ formula, where M is divalent cation like Co^{2+} , Ni^{2+} , Mn^{2+} , Cu^{2+} , Mg^{2+} , Zn^{2+} . Here, parenthesis and square brackets represent tetrahedral and octahedral sites respectively. In the normal spinel, the tetrahedral sites are occupied by divalent cations while trivalent cations occupy octahedral sites. In contrast, divalent cations occupy octahedral sites in inverse spinel, whereas trivalent cations are distributed equally among A-and B-sites.. The degree of inversion x is the proportion of the trivalent cation Fe^{3+} occupying tetrahedral sites [5,6]. The crystal structure of a ferrite can be regarded as an interlocking network of positively charged metal ions and negatively charged divalent oxygen ions. In spinel ferrites, the relatively large oxygen anions form a cubic close packing with $\frac{1}{2}$ of the octahedral and $\frac{1}{8}$ of the tetrahedral interstitial sites occupied by metal ions.

The spinel AB_2O_4 (where A is one or more divalent cation and B is one or more trivalent cation) structure can be generally described as a cubic close pack arrangement of oxygen ions in which tetrahedral A and octahedral B interstitial lattice sites are occupied by cation [7].

Nano ferrites were usually prepared by the conventional ceramic methods but the resultant products are not necessarily always stoichiometric or homogeneous [8]. A variety of chemical synthesis methods such as co-precipitation, hydrothermal synthesis, and sol-gel process have been developed. [9-10]. The Citrate-gel auto combustion technique has been used for the preparation of mixed nano crystalline spinel ferrites with specific properties, such as controlled stoichiometry and narrow particle size distribution. The low cost, simplicity and short time of production and the purity and homogeneity of final product are included among its advantages [5].

In the present work we reported the results of synthesis and structural properties of $Mn_xCo_{1-x}Fe_2O_4$ ferrites prepared by non conventional citrate gel auto combustion method.

II. Experimental details

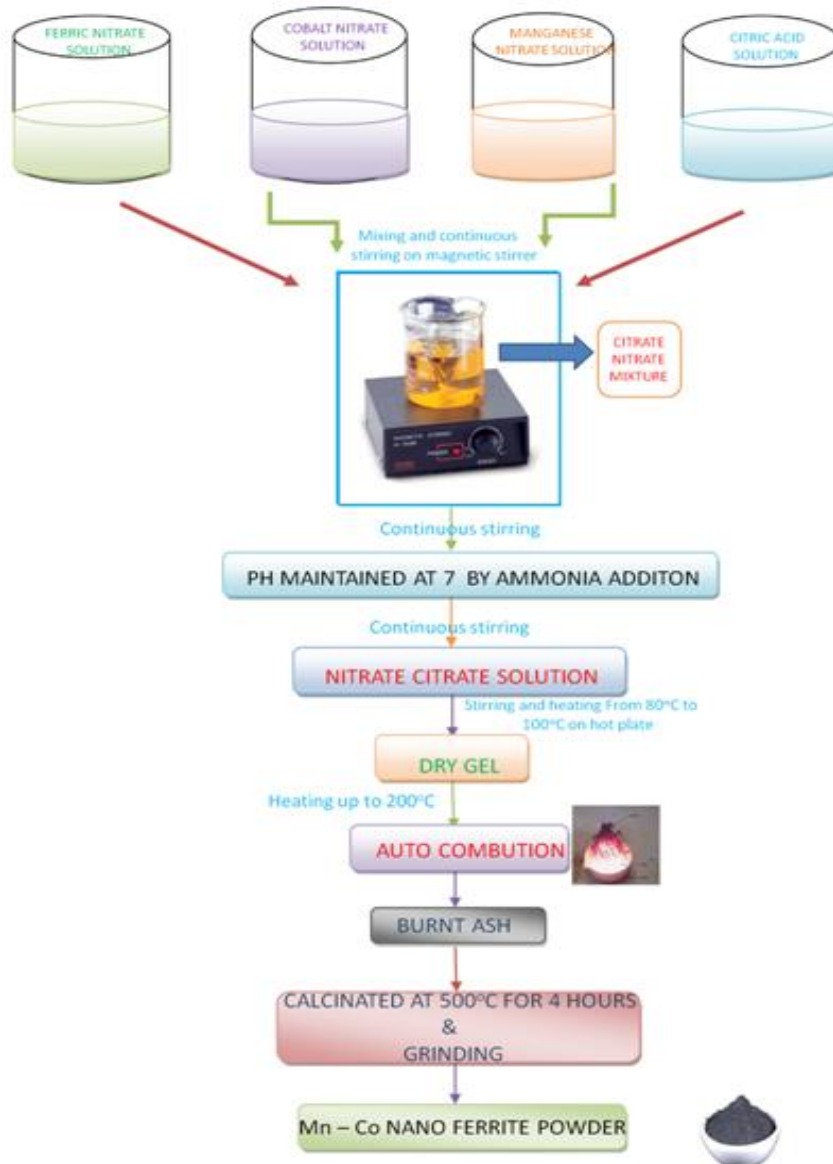
The manganese substituted cobalt nano ferrite particles having the general formula $Mn_xCo_{1-x}Fe_2O_4$ (where $x=0.0,0.2,0.4,0.6,0.8,10$) were synthesized by citrate-gel auto combustion technique a very low temperature ($180^\circ C$) using the below mentioned raw materials.

S.No	ChemicalName	Purity (%)	Manufacturer name	Place of Manufacture
1	Manganese-nitrate ($Mn(NO_3)_2 \cdot 6H_2O$)	98.8	SIGMA-ALDRICH	Sprucestreet, St.Louis, USA
2	Ferric-nitrate ($Fe(NO_3)_3 \cdot 9H_2O$)	99	Sdfine-CHEM LIMITED	Mumbai, India.
3	Cobalt-nitrate ($Co(NO_3)_2 \cdot 6H_2O$)	99	Sdfine-CHEM LIMITED	Mumbai, India.
4	Citric-acid ($C_6H_8O_7 \cdot H_2O$)	99.7	Sdfine-CHEM LIMITED	Mumbai, India.
5	Ammonia solution (NH_3).	99.7	Sdfine-CHEM LIMITED	Mumbai, India.

III. Synthesis:

Required quantities of metal nitrates were dissolved in a minimum quantity of distilled water and mixed together. Aqueous solution of Citric acid was then added to the mixed metal nitrate solution. Ammonia solution was then added with constant stirring to maintain PH of the solution at 7. The resulting solution was continuously heated on the hot plate at $100^\circ C$ up to dryness with continuous stirring. A viscous gel has resulted. Increasing the temperature up to $200^\circ C$ lead the ignition of gel. The dried gel burnt completely in a self propagating combustion manner to form a loose powder. The burnt powder was ground in Agate Mortar and Pestle to get a fine ferrite powder. Finally the burnt powder was calcinated in air at $500^\circ C$ temperature for four hours and cooled to room temperature.

Chemical Reaction:



IV. Calculations

Using the X-ray diffraction data, the crystallite size of the synthesized samples was calculated using maximum intensity peak from Scherrer's formula [11] as mentioned below

$$\text{Crystallite size} = D = \frac{0.91 \lambda}{\beta \cos \theta}$$

Where λ = the wavelength of X-ray

β = Full width and half maxima in radians, θ = Bragg's angle at the peak position

Lattice parameter 'a' of the individual composition can be calculated using the following expression [11]:

$$a = d \sqrt{h^2 + k^2 + l^2}$$

Where a is lattice parameter, d is inter planar distance, h k l is miller indices The X-ray density (dx) is calculated using the following relation

$$x\text{-ray density} = dx = \frac{8M}{Na^3} \text{ gm/cc}$$

Where M is molecular weight of the sample, N is Avogadro number, a is lattice parameter Volume of the unit cell 'V' is calculated using the following expression [11]:

$$v = a^3$$

The distance between the magnetic ions (hoping length) on A-site(Tetrahedral) and B site(Octahedral) is calculated according to the following relations

$$dA = 0.25a\sqrt{3} \quad \text{and} \quad dB = 0.25a\sqrt{2} \quad [12]$$

Where 'a' is the lattice parameter

V. Results and Discussions

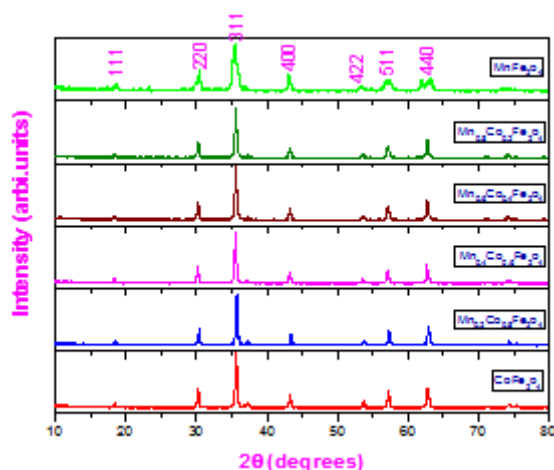
X-ray diffraction technique was used to confirm the formation of single phase cubic spinel ferrites; all the samples demonstrate the high crystalline structure. The samples show all the characteristic reflections of ferrite material with most intense (3 1 1) reflection which confirms the formation of cubic spinel structure (Fig. 3). The XRD patterns were indexed using the JCPDS card Nos. 22-1086 [13] and 74-2403 [14]. The Mn concentration dependence of the lattice constant a, determined from XRD data, for x = 0.0 to x = 1.0, is given in Table 2. From Fig. 1 it is observed that the lattice constant gradually increases from 8.318Å to 8.385Å with increasing Mn²⁺ content, obeying Vegard's law [15]. Usually, in a solid solution of spinels

within the miscibility range, a linear change in the lattice constant with the concentration of the components is observed [16,17]. This linear increase in lattice constant may be attributed to the replacement of smaller Co²⁺ (0.78 Å) and Fe³⁺ (0.64 Å) ions by the larger Mn²⁺ (0.83 Å) ions in the Co_{1.2-x}Mn_xFe_{1.8}O₄ system [18]. Similar variation of lattice parameter is reported by Zhou et al. for the thin film samples of CoFe_{2-x}Mn_xO₄ [19]. The theoretical density was estimated by using the relation [20],

$$D_x(\text{ferrite}) = \frac{8M}{N \times a^3}$$

where, M is molecular weight of the ferrite, N is the Avogadro's number and a³ is the volume of the cubic unit cell. It was observed that the theoretical density decreases with increasing Mn content in the cobalt ferrite matrix which may be attributed to the ionic radii of constituent ions causing increase in lattice constant and the densities of pure CoFe₂O₄ (5.29 g/cm³) and pure MnFe₂O₄ (4.98 g/cm³).

The calculated values of crystalline size for the different compositions are given in the table(1). It can be seen from the table that the values of the crystal size varies from 11nm to 33nm. The crystalline size was not same for all Mn concentrations because the preparation condition followed here which gave rise to different rate of ferrite formation for different concentrations of Mn, favouring the variation of crystalline size. Conventional methods needs to high temperatures and more time, but in this method, ferrite phase can be produced very fast at low temperature



Fig(1): XRD Pattern of Mn-Co Nano ferrites

VI. Morphological analysis

Micro structural analysis (surface morphology) of the prepared samples was carried out by scanning Electron microscopy (SEM). The SEM micrographs of as synthesized samples were obtained to study to the morphology and microstructure of the samples. Figure 2 shows the morphological changes of the compacted ferrite by Mn doping in CoFe_2O_4 system ($0 \leq x \leq 1.0$). The microstructural features clearly show that the morphology is affected by the dopant, i.e. (i) the mode of fracture changes from predominantly trans granular in the un doped sample to predominantly inter granular in the Mn^{2+} doped ones and (ii) the grain size increases from the un doped sample to Mn^{2+} doped samples. Furthermore, Mn^{2+} doping tends to change the initial shape of the grains. It is evident from Figure ($x=0$) that the un doped specimen showed a well-densified microstructure with faceted crystallites and many residual pores. By incorporating Mn^{2+} , the average grain size increased, the crystallites tend to a tubular shape and boundaries become clean and thinner (Figure ($x=0.6$ and 1.0)).

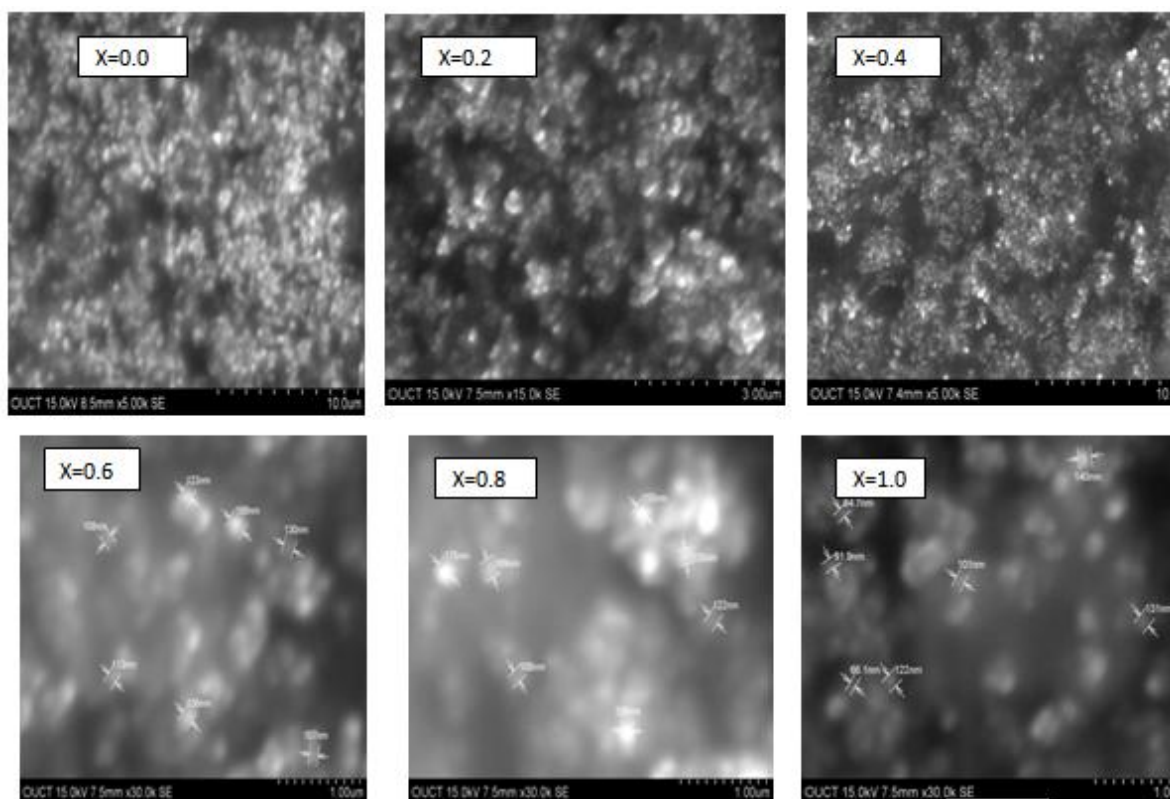


Fig.(2) SEM Diagrams of Mn-Co Nano Ferrites

VII. Elemental Analysis by EDS :

The elemental analysis of all the Mn-Co nano ferrite samples with different composition was analyzed by an Energy Distribution Spectrometer (EDS) and the weight % and atomic % of various elements in the samples were shown in **Table.(1)**

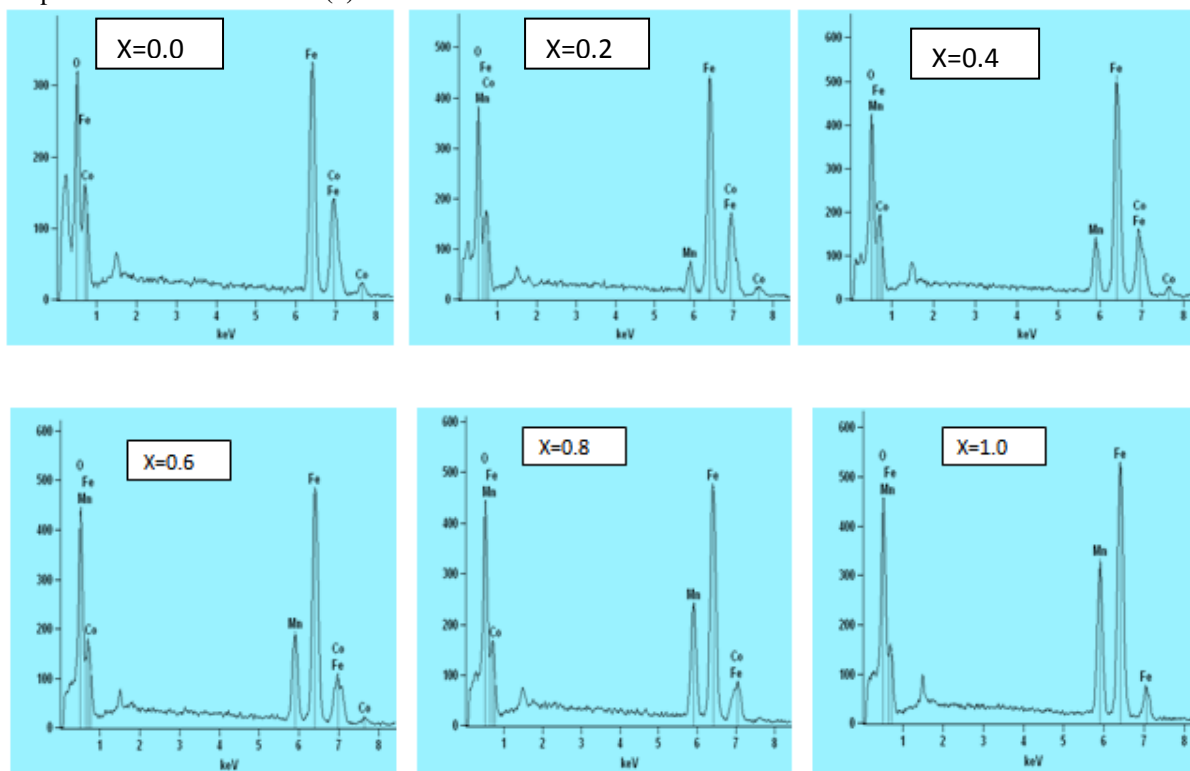


Fig.3 EDS Diagrams of Mn-Co Nano Ferrites

Element	O		Fe		Co		Mn	
	Weight %	Atomic %						
CoFe ₂ O ₄	16.82	41.80	55.45	39.50	27.72	18.70	-	-
Mn _{0.2} Co _{0.8} Fe ₂ O ₄	14.56	37.64	54.32	40.22	25.35	17.80	5.77	4.34
Mn _{0.4} Co _{0.6} Fe ₂ O ₄	13.59	35.65	57.30	43.05	17.95	12.77	11.15	8.53
Mn _{0.6} Co _{0.4} Fe ₂ O ₄	14.53	37.33	55.74	41.01	11.85	8.26	17.88	13.40
Mn _{0.8} Co _{0.2} Fe ₂ O ₄	15.02	38.17	54.94	39.98	7.93	5.46	22.12	16.39
MnFe ₂ O ₄	14.74	37.48	50.76	36.96	-	-	24.50	25.56

Table(1).Elements of each sample composition analysed by % of weight and atomic % obtained by EDS

Sl. No	Composition	Molecular weight	Particle size(D) nm	Lattice parameter A°	X-ray Density gm/cc	Volume(A°) ³	A-site(dA)	B-site(dB)
1	CoFe ₂ O ₄	234.623	33.4	8.318	5.195	575.67	3.602	2.941
2	Mn _{0.2} Co _{0.8} Fe ₂ O ₄	233.824	31.6	8.343	5.276	580.75	3.612	2.949
3	Mn _{0.4} Co _{0.6} Fe ₂ O ₄	233.025	33.6	8.350	5.279	582.25	3.615	2.952
4	Mn _{0.6} Co _{0.4} Fe ₂ O ₄	232.226	33.7	8.351	5.346	582.55	3.616	2.952
5	Mn _{0.8} Co _{0.2} Fe ₂ O ₄	231.427	36.6	8.359	5.352	584.24	3.619	2.955
6	MnFe ₂ O ₄	230.628	11.5	8.385	5.376	589.58	3.630	2.964

Table (2).Values of the Crystalline size, Lattice parameter(a), X-ray density(dx), volume, A-site and B-site

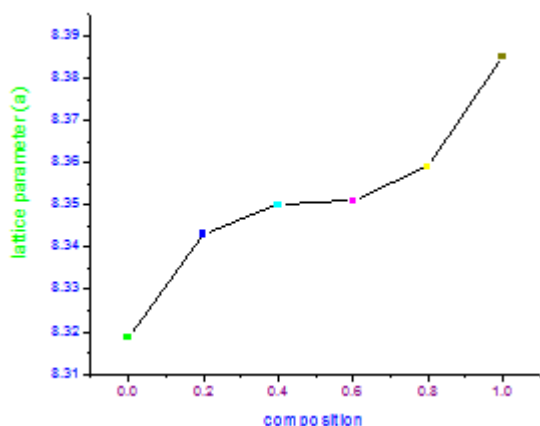


Fig.4. lattice parameter Vs compositions

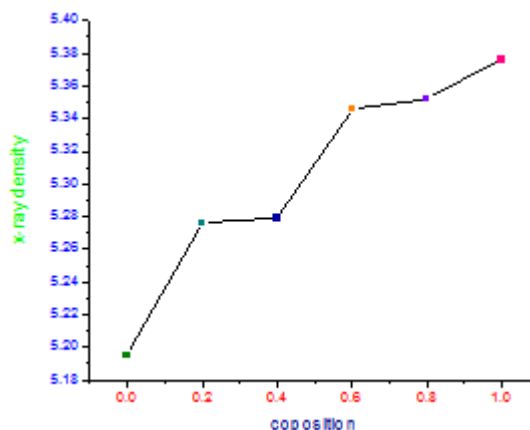


Fig.5. X-ray density Vs compositions

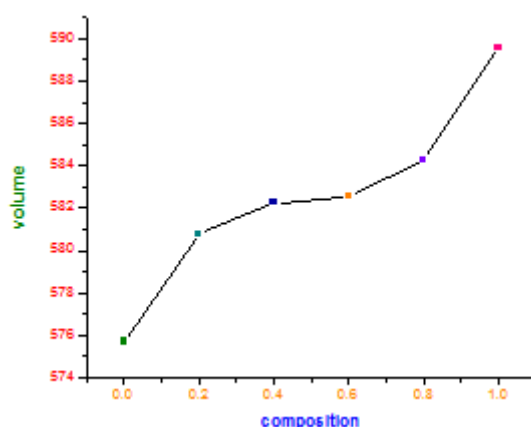


Fig.6. volume Vs compositions

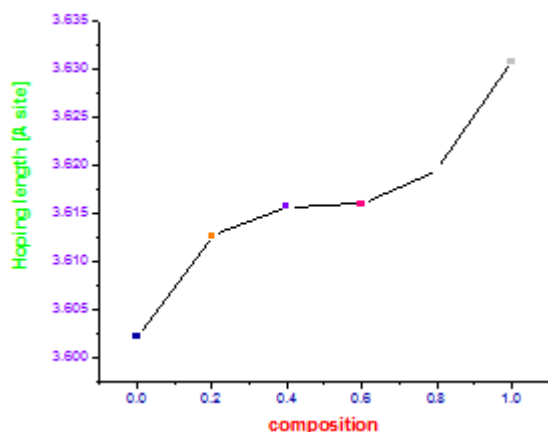


Fig.7. Hoping length(dA) Vs compositions

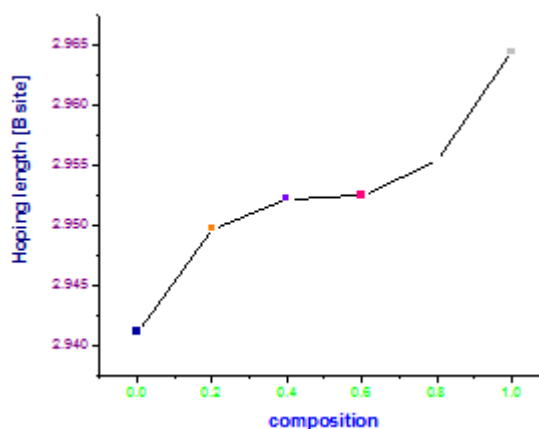


Fig.8. Hoping length(dB) Vs compositions

A plot of the lattice parameter Vs compositions is shown in **Fig.1**, which indicates the variation of lattice parameter with composition. The lattice parameter is found to increases linearly with increase of Mn ions in the Mn-Co nano-ferrites system indicating that the system obeys Vegard's law [17]. The increase in lattice parameter with increase in Mn²⁺ content is explained on the basis of the relative ionic radii of Mn²⁺ and Co²⁺ ions. This linear increase in lattice constant may be attributed to the replacement of smaller Co²⁺ (0.78 Å) and Fe³⁺ (0.64 Å) ions by the larger Mn²⁺ (0.83 Å) increase in the lattice parameter[20]. The x-ray density (dx) is calculated using the following formula [13] and were tabulated in Table 2.

$$Dx(\text{ferrite}) = \frac{8M}{N \times a^3}$$

where M=Molecular weight of the sample, N = Avagadro number, and a= lattice parameter.

A plot of the x-ray density (dx) Vs compositions is shown in **Fig.2** The X-Ray density depends on the lattice parameters.. From the plot it is observed that X-Ray density increase with increase in Mn content (x), this is because the decrease in mass overtakes the decrease in volume of unit cell. Hence X-Ray density is increased with increase in Mn content.

Volume of the unit cell is calculated as $V=a^3$ The calculated values are tabulated in **Table 2**. It is observed that volume of this unit cell increases with increase in Mn content(**Fig.6**). It is because Volume of the unit cell depends on the lattice parameter which increases with increase in Mn content.

The distance between magnetic ions (hopping length) in A site (Tetrahedral) and B site (Octahedral) were calculated by using the following relations [13]. $dA= 0.25a\sqrt{3}$ and $dB= 0.25a\sqrt{2}$ Where 'a' is lattice parameter The values of the Hopping length for tetrahedral site (dA) and octahedral (dB) were tabulated in **Table2**.

VIII. Conclusion

Mn-Co nano ferrites with the chemical composition $Mn_xCO_{1-x}Fe_2O_4$ ($x=0.0, 0.2,0.4,0.6,0.8,1.0$)were successfully prepared by Citrate gel auto-combustion technique with a crystallite size ranging from 11 to 33nm. X-ray diffraction studies confirmed the formation of single phased cubic spinel structure of the ferrites without any impurity peak. The nitrate ions play an important role in the auto-combustion of nitrate-citrate dried gel. The combustion process is an oxidation-reduction reaction, in which the NO_3^{-1} ion is an oxidant and the carboxyl group is the reductant. The lattice parameters are increases with the increase of Mn substitution in Mn-Co ferrites which indicates that the mixed Mn-Co nano-ferrite system obeys Vegard's Law. The SEM analysis reveals the large agglomeration of the nanoparticles. EDS data gives the elemental % and atomic % in the mixed Mn-Co ferrites and it shows the presence of Mn, CO, Fe and O without precipitating cations.

Acknowledgements

The authors are very grateful to Prof.L.N.SHARADHA, Head, Department of Chemistry,Prof.V.UMA, DEAN, university College of Science, Osmania University, Hyderabad. And Prof.N.SAILU, Principal, University College of technology, osmania university, Hyderabad for their encouragement in research work.

References

- [1]. A. Henglein, Chem. Rev. 89 (1989) 1861.
- [2]. H. Weller, Angew. Chem. Int. Ed. Engl. 32 (1993) 41.
- [3]. A.P. Alivisatos, J. Phys. Chem. 100 (1996) 13226.
- [4]. C.C. Chen, A.B. Herhold, C.S. Johnson, A.P. Alivisatos, Science 276 (1997) 389.
- [5]. C. Kittel, Introduction to Solid State Physics, 7th ed., John Willey & Sons, New York, 2004.
- [6]. A. Goldman, Modern Ferrite Technology, 2nd ed., Springer Science BusinessMedia, Inc., New York,2006.
- [7]. B.D. Cullity, Elements of X-ray Diffraction, Addison-Wesley Publishing Com-pany, USA, 1956
- [8]. V.K. Sharma, J.O. Smith, F.J. Millero, Environ. Sci. Technol. 31 (1997) 2486.
- [9]. D.W. Hwang, H.Y. Ko, J.H. Lee, H.Kang, S.H. Ryu, J.C. Song, D.S.Lee, S. Kim, J.Nucl.Med.51(2010)98.
- [10]. A. Kondo, H. Fukuda, J. Ferment, Bioengineering 84 (1997) 337-341.
- [11]. M.K. Shobana, S.Sankar, V. Rajendran, J. Mater. Chem. Phys. 113 (2009) 10.
- [12]. B.Vishvanathan, V.R.K.Murthy,Ferrite Materials Science and Technology, narosa Public House,New Delhi (1990)
- [13]. Natl.Bur.Stand. (U.S) Monogr. 25 (1971) 22.
- [14]. U. KÖnig, G. Chol, J. Appl. Crystallogr. 1 (1968) 124.
- [15]. S.S. Bhatu, V.K. Lakhani, A.R. Tanna, N.H. Vasoya, J.U. Buch, P.U. Sharma, U.N. Tridevi, H.H. Joshi, K.B. Modi, Ind. J. Pure Appl. Phys. 45 (2007) 596.
- [16]. C.G. Whinfrey, D.W. Eckart, A. Tauber, J. Am. Chem. Soc. 82 (1960) 2695.
- [17]. N.H. Vasoya, V.K. Lakhani, P.U. Sharma, K.B. Modi, Ravi Kumar, H.H. Joshi, J.Phys.: Condens. Matter 18 (2006) 8063.
- [18]. K.J. Standley, Oxide Magnetic Materials, Clarendon Press, Oxford, 1972.
- [19]. B. Zhou, Y.-W. Zhang, C.-S. Liao, C.-H. Yan, J. Magn. Magn. Mater. 247 (2002) 70.
- [20]. J. Smith, H.P. Wijn, Ferrites, Wiley, New York, 1959.